ISSN 1070-3284, Russian Journal of Coordination Chemistry, 2022, Vol. 48, No. 4, pp. 233–241. © Pleiades Publishing, Ltd., 2022.
Russian Text © The Author(s), 2022, published in Koordinatsionnaya Khimiya, 2022, Vol. 48, No. 4, pp. 238–247.

o-Benzoquinone Cobalt Complexes Bearing Organosilicon Radicals: Quantum-Chemical Study

A. A. Starikova[a, *], **M. G. Chegerev**[a], **A. G. Starikov**[a], **and V. I. Minkin**[a]

[a] *Institute of Physical and Organic Chemistry, Southern Federal University, Rostov-on-Don, Russia*

**e-mail: aastarikova@sfedu.ru*

Received September 24, 2021; revised October 14, 2021; accepted October 15, 2021

Abstract—A computer modeling (DFT UTPSSh/6-311++G(d,p)) of electronic structures, geometric parameters, energy characteristics, and magnetic properties of the mononuclear cobalt complexes with tetradentate N-donor bases (tris(2-pyridylmethyl)amines and *N*,*N*′-dialkyl-2,11-diaza[3.3]-(2,6)pyridinophanes) and *o*-benzoquinones comprising triangulene organosilicon radicals was performed. Paramagnetism of all states of the studied molecules is predicted. It is ascertained that the electronic configurations and energy characteristics of the isomers of the complexes under study are controlled by alkyl substituents in the ancillary N-donor ligands. The compounds capable of manifesting thermally initiated spin state switching rearrangements via spin-crossover and valence tautomerism mechanisms are revealed.

Keywords: cobalt complexes, *o*-benzoquinone, N-donor bases, organosilicon polycyclic compounds, density functional theory

DOI: 10.1134/S1070328422040054

INTRODUCTION

Rapidly increasing interest in coordination compounds that demonstrate spin state switching due to external effects (temperature, pressure, and irradiation) is observed in the recent decades [1–9]. These magnetically active metal complexes can exist as two or more electronic isomers (electromers [10]) with diverse magnetic properties, which allows their manifold applications in devices of molecular electronics and spintronics [1–4, 7, 11–15]. Numerous studies are devoted to the search for promising bi- and polystable molecules [2–9, 12–20].

Spin-crossover (SCO) is among the most abundant mechanism of magnetic bistability and represents a change in the spin state of the coordinated metal ion induced by external factors and caused by the rearrangement of electrons inside the valence shell [21, 22]. The strength of the ligand field appropriate for the SCO to occur is achieved in transition metal compounds with the electronic configurations d^4–d^7, in particular, in the iron(II/III) [23–27] and cobalt(II) [28–30] complexes with N-donor ligands. Another method for spin state switching in coordination compounds is valence tautomerism (VT), or redox isomerism, including the reversible intramolecular electron transfer between the metal center and redox-active ligand [31, 32]. This phenomenon was comprehensively studied for the cobalt complexes with the *o*-benzoquinone derivatives, and there are examples of VT transitions in the compounds of some other *d* metals [32, 33], lanthanides [34], and main group elements [35, 36].

Heterospin magnetically active compounds with two or more different paramagnetic centers are attractive objects from the viewpoint of molecular magnetism. Complexes of transition metals with open electronic shells including additional spin carriers (ligands and/or functional groups) are of special interest [18, 37–46]. *o*-Benzoquinone in the semiquinone (SQ) form is a classical example of the radical ligand. The previous experimental [47–51] and theoretical [50–54] studies showed that the *o*-benzoquinone cobalt complexes with N-donor tetradentate bases can demonstrate SCO ($_{LS}Co^{II}$–SQ $\rightleftarrows$ $_{HS}Co^{II}$–SQ) and VT ($_{LS}Co^{III}$–Cat $\rightleftarrows$ $_{HS}Co^{II}$–SQ) rearrangements (Cat is the dianionic catecholate form of *o*-benzoquinone). Similar compounds bearing a stable radical (1,2,3,5-dithiadiazolyl, 1,5-dimethyl-6-oxoverdazyl, nitronyl nitroxide, and TEMPO) in the fourth position of the quinone ring were constructed in order to impart paramagnetic properties to the diamagnetic electromer $_{LS}Co^{III}$–Cat [55, 56]. According to the quantum-chemical calculation results, the nature and method of attachment of the considered radical substituents exert no substantial effect on the ability of the cobalt complexes to manifest magnetic bistability induced by different mechanisms.

We have recently studied theoretically a series of VT adducts of cobalt bis(diketonates) with the *o*-benzoquinone ligands comprising the triangulene fragments [57–60]. An advantage of these systems over the earlier proposed heteroligand complexes [6, 61–63] is the unique ability of triangulenes [64] and their heavy analogs [65] to increase the number of unpaired electrons with an increase in the number of six-membered rings (n) in the triangle base (Scheme 1) [66, 67] due to which the total spin of the system can be increased by the expansion of the polycyclic moiety. The obtained calculation results [57–60] indicate an insignificant effect of doping of the hydrocarbon polycyclic fragment by the silicon or germanium atoms on the energy parameters of the isomers and character of exchange coupling. Selected paramagnetic triangulene derivatives are shown in Scheme 1.

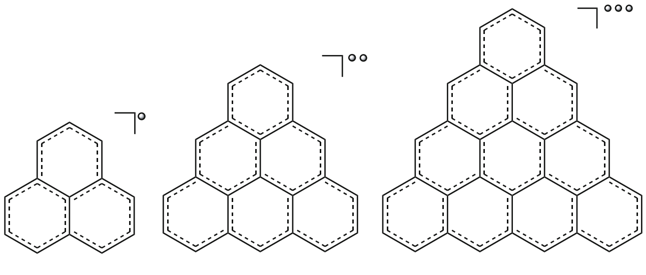
$n = 2$ $n = 3$ $n = 4$

Scheme 1.

The computer modeling of coordination compounds **I–IV** (Scheme 2) with different numbers of six-membered rings in the base of the triangular polycycle ($n = 2–4$) was performed in this work to search for new polyspin systems prone to switching magnetic properties via the SCO and/or VT mechanism. *N*,*N*'-Di-*iso*-propyl-2,11-diaza[3.3]-(2,6)pyridinophane, *N*,*N*'-di-*tert*-butyl-2,11-diaza[3.3]-(2,6)pyridinophane, and tris(2-pyridylmethyl)amine (TPA) derivatives containing two or three CH_3 groups in the pyridine rings were chosen as tetradentate N-donor bases according to the available experimental data indicating a possibility of spin transitions to occur in the cobalt complexes with this ligand environment [47–51]. In turn, hexafluorophosphate anions are widely used for the synthesis of similar salt-like *o*-benzoquinone cobalt complexes with the nitrogen-containing ligands [51].

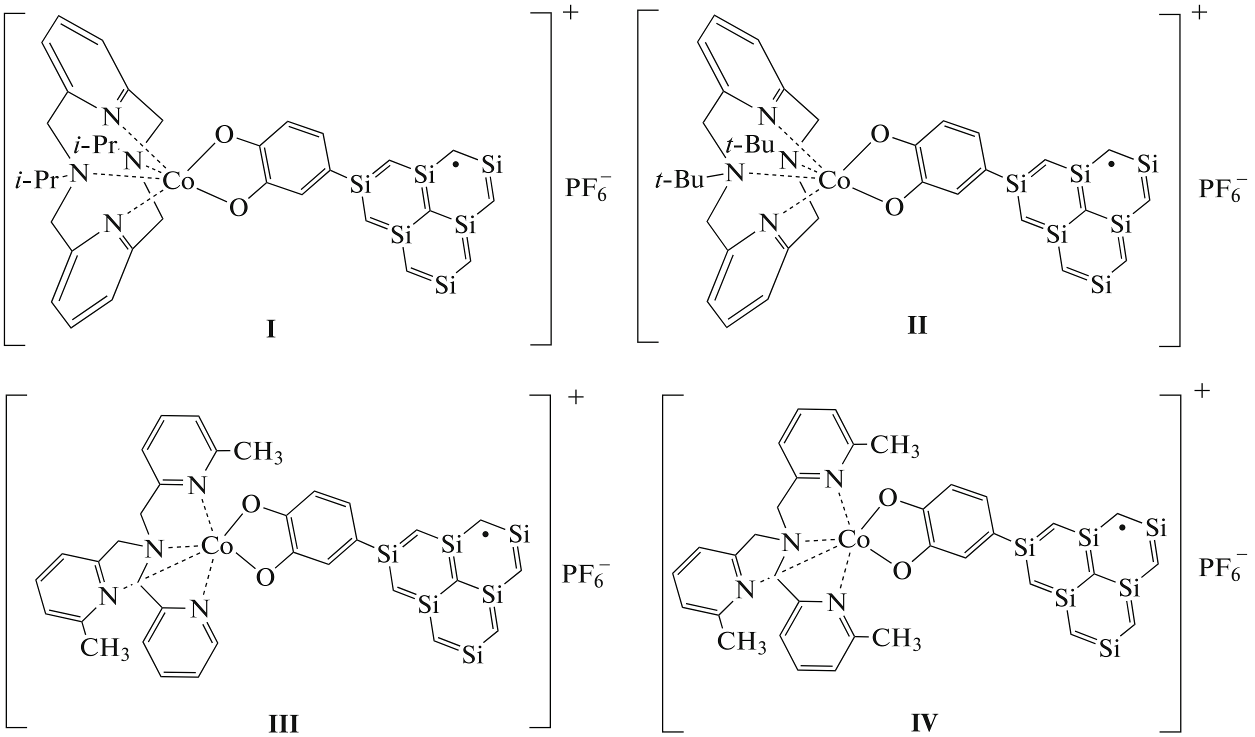

I **II** **III** **IV**

Scheme 2.

EXPERIMENTAL

Calculations were performed using the Gaussian 16 software [68] by the density functional theory (DFT) with the UTPSSh functional [69, 70] and 6-311++G(d,p) extended basis set, the combination of which correctly reproduces the energy and magnetic characteristics of the complexes exhibiting magnetic bistability [50, 52, 71–74]. According to the calculation results obtained in this approximation for the experimentally studied cobalt compounds, SCO occurs at $\Delta E_{\text{HS-LS}} < 6$ kcal/mol, and VT takes place at $\Delta E_{\text{HS-LS}} < 8$ kcal/mol [50]. It was shown that outer-sphere counterions should be taken into account in the DFT study of the transition metal complexes with the redox-active ligands [75]. Therefore, in this study the quantum-chemical calculations were performed for the compounds comprising the hexafluorophosphate anion, the position and orientation of which were taken from the XRD data for the structurally similar compounds [51]. Stationary points were localized on the potential energy surface (PES) by the full geometry optimization of molecular structures followed by checking the stability of the DFT wave function and calculation of the force constants. Exchange interaction parameters (J, cm^{-1}) were calculated in terms of the broken symmetry (BS) formalism [76] using the Yamaguchi general spin projection approach [77]. Graphical images of the molecular structures were drawn using the ChemCraft software [78].

RESULTS AND DISCUSSION

According to the calculation results, the minimum on the doublet PES in which the single lone electron is delocalized over the organosilicon fragment corresponds to the ground state of complex **I** (n = 2) (Fig. 1). The coordination bond lengths (Table 1) and the absence of a spin density in the quinone ring and on the metal center make it possible to unambiguously ascribe the electronic configuration ${}_{\mathrm{LS}}\mathrm{Co}^{\mathrm{III}}$–Cat–X, where X is the polycyclic organosilicon radical, to this electromer. The high-spin form of compound **I** (n = 2) is presented by a minimum on the sextet PES. The spin density distribution shown in Fig. 1 and calculated geometric characteristics indicate that the discussed ${}_{\mathrm{HS}}\mathrm{Co}^{\mathrm{II}}$–SQ–X electromer comprises three paramagnetic centers: the high-spin divalent cobalt ion, radical anion SQ form of *o*-benzoquinone, and polycyclic fragment. As follows from the steric structures of the isomers of complex **I** (n = 2), the polycyclic fragment lies in the same plane with the quinone ring (Fig. 1). Remarkably, when the starting geometry with the perpendicular arrangement of the organosilicon radical is specified, structure optimization results in the turn of X by 90° and formation of the single conjugated Cat/SQ–X π system. The destabilization of the high-spin isomer ${}_{\mathrm{HS}}\mathrm{Co}^{\mathrm{II}}$–SQ–X by more than 10 kcal/mol (Table 2) indicates that complex **I** (n = 2) would be in the ground doublet state ${}_{\mathrm{LS}}\mathrm{Co}^{\mathrm{III}}$–Cat–X without any signs of the VT transition.

The quantum-chemical study of compounds **I** (n = 3, 4) showed that an increase in the number of six-membered rings in the organosilicon fragment was not accompanied by a change in the electronic configurations of the found isomers and bond lengths in the coordination site (Table 1). The differences in energies between the electromers of complexes **I** (n = 3, 4) are close to ΔE found for compound **I** (n = 2) and are equal to 11.8 kcal/mol (Table 2). Taking into account the spin-forbidden character of the VT process and a necessity of surmounting the energy barrier for the transition ${}_{\mathrm{LS}}\mathrm{Co}^{\mathrm{III}}$–Cat–X $\rightleftarrows$ ${}_{\mathrm{HS}}\mathrm{Co}^{\mathrm{II}}$–SQ–X, we can assert that the probability of the intramolecular electron transfer in the systems discussed is very low. Therefore, complexes **I** (n = 3, 4) will be presented by the low-spin electromers ${}_{\mathrm{LS}}\mathrm{Co}^{\mathrm{III}}$–Cat–X in a wide temperature range. The polycyclic fragments of compounds **I** (n = 3, 4) contain two and three lone electrons, respectively, which can be considered as a single paramagnetic center due to strong ferromagnetic exchange interactions inside the organosilicon radical [66, 79–81].

A comparison of the calculation data for compounds **I** (n = 2–4) with the earlier obtained results of studying the *o*-benzoquinone cobalt complexes bearing *N*,*N'*-di-*iso*-propyl-2,11-diaza[3.3]-(2,6)pyridinophane [50, 55] shows an increase in the difference in energies between the electromers in the systems with organosilicon polycycles. The predicted increase in the stability of the ${}_{\mathrm{LS}}\mathrm{Co}^{\mathrm{III}}$–Cat–X isomers can be explained by the energy preference of the formation of the generalized π system between triangulene X and the aromatic Cat fragment, whereas the conjugation with SQ, which is not aromatic, does not give a comparable energy gain. The numeration of atoms in the coordination site of complexes **I**–**IV** is shown in Scheme 3.

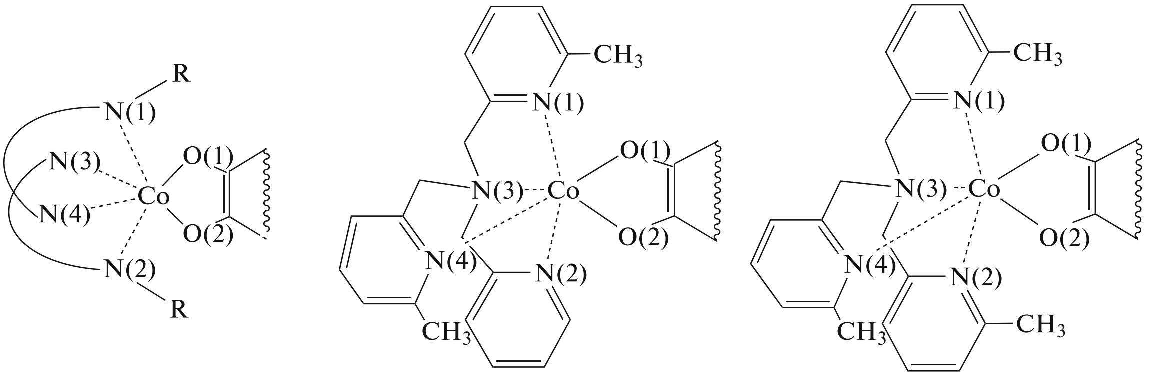

I, **II** (R = *i*-Pr, *t*-Bu) **III** **IV**

Scheme 3.

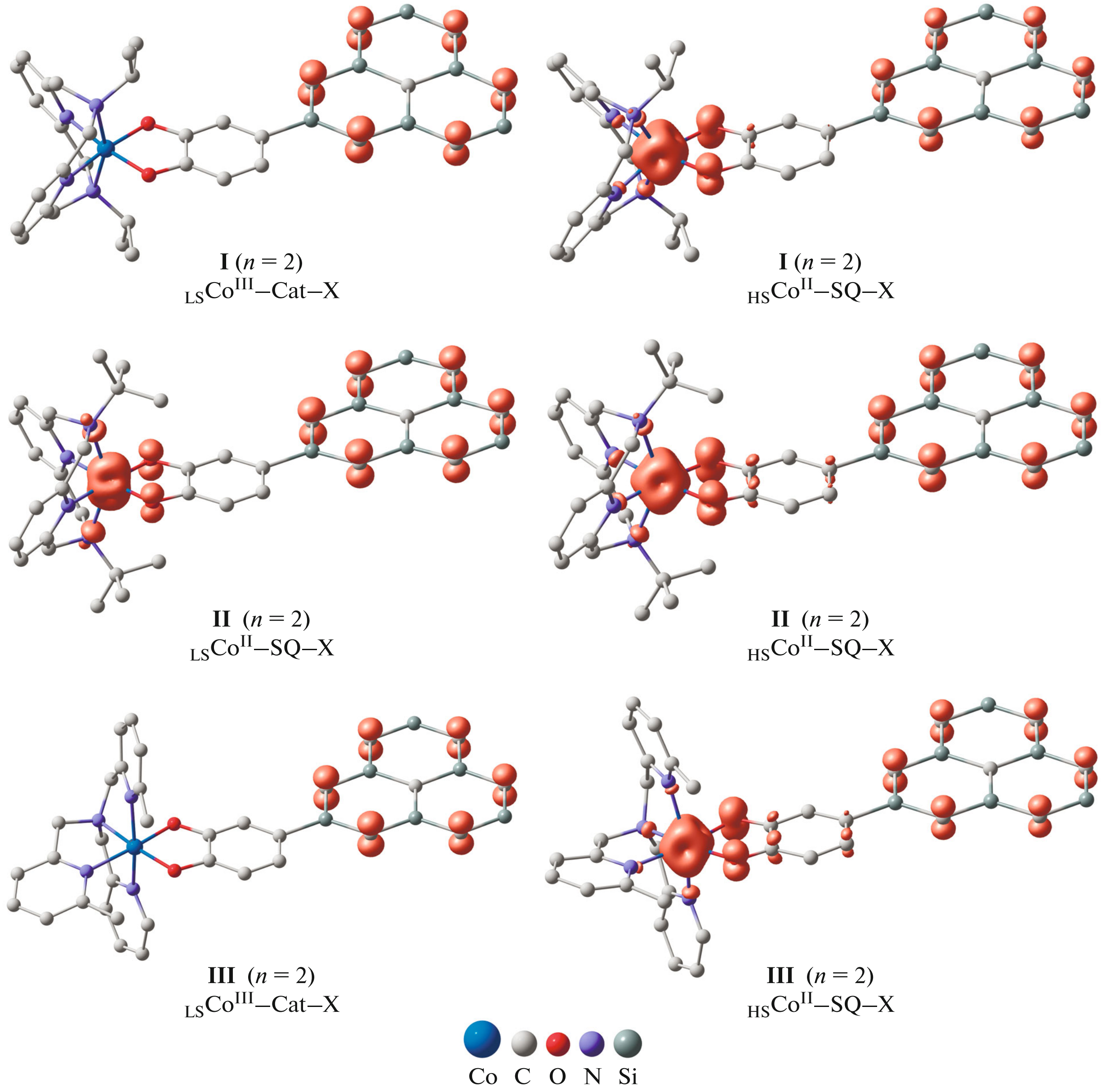

I ($n = 2$)
$_{LS}Co^{III}$–Cat–X

I ($n = 2$)
$_{HS}Co^{II}$–SQ–X

II ($n = 2$)
$_{LS}Co^{II}$–SQ–X

II ($n = 2$)
$_{HS}Co^{II}$–SQ–X

III ($n = 2$)
$_{LS}Co^{III}$–Cat–X

III ($n = 2$)
$_{HS}Co^{II}$–SQ–X

Fig. 1. Steric structures and spin density distribution in the electromers of complexes **I**–**III** ($n = 2$) calculated by the DFT UTPSSh/6-311++G(d,p) method. Hydrogen atoms and outer-sphere counterions are omitted, and the contour value is 0.02 e/Å^3.

The replacement of the isopropyl substituents at the nitrogen atoms by *tert*-butyl groups expectedly results [50, 51, 55] in the situation where the $_{LS}Co^{II}$–SQ–X electromers comprising the low-spin divalent cobalt ion and SQ radical anion are the most stable forms of compounds **II** (n = 2–4) (Fig. 1, Table 1). Regardless of the number of six-membered rings in the organosilicon radical, the high-spin isomers are destabilized relative to the ground state by 7.9 kcal/mol (Table 2). The predicted values somewhat exceed the range of values characteristic of SCO [50] indicating the possibility of incomplete SCO transitions $_{LS}Co^{II}$–SQ–X $\rightleftarrows$ $_{HS}Co^{II}$–SQ–X to occur in complexes **II** (n = 2–4).

The study of exchange interactions in the $_{LS}Co^{II}$–SQ–X electromers indicates a strong ferromagnetic coupling in the $_{LS}Co^{II}$–SQ and SQ–X pairs, and the exchange between the metal center and polycyclic fragment is nearly absent due to their remoteness (Table 3). The high-spin $_{HS}Co^{II}$–SQ–X electromers are characterized by a moderate antiferromagnetic coupling of spins of lone electrons in $_{HS}Co^{II}$ and SQ, and the J_2 and J_3 parameters are close to those found

Table 1. Coordination bond lengths (Å) in the electromers of complexes **I**–**IV** (n = 2–4) calculated by the DFT UTPSSh/6-311++G(d,p) method

Complex	Electromer	Co–O(1)*	Co–O(2)	Co–N(1)	Co–N(2)	Co–N(3)	Co–N(4)
I (n = 2)	${}_{\mathrm{LS}}\mathrm{Co}^{\mathrm{III}}$–Cat–X	1.888	1.884	2.045	2.045	1.874	1.872
	${}_{\mathrm{HS}}\mathrm{Co}^{\mathrm{II}}$–SQ–X	2.040	2.027	2.281	2.282	2.036	2.033
I (n = 3)	${}_{\mathrm{LS}}\mathrm{Co}^{\mathrm{III}}$–Cat–X	1.890	1.883	2.048	2.043	1.873	1.872
	${}_{\mathrm{HS}}\mathrm{Co}^{\mathrm{II}}$–SQ–X	2.039	2.026	2.284	2.278	2.035	2.032
I (n = 4)	${}_{\mathrm{LS}}\mathrm{Co}^{\mathrm{III}}$–Cat–X	1.890	1.884	2.048	2.044	1.873	1.872
	${}_{\mathrm{HS}}\mathrm{Co}^{\mathrm{II}}$–SQ–X	2.039	2.026	2.284	2.277	2.035	2.032
II (n = 2)	${}_{\mathrm{LS}}\mathrm{Co}^{\mathrm{II}}$–SQ–X	1.881	1.873	2.346	2.356	1.929	1.928
	${}_{\mathrm{HS}}\mathrm{Co}^{\mathrm{II}}$–SQ–X	2.039	2.031	2.353	2.371	2.038	2.037
II (n = 3)	${}_{\mathrm{LS}}\mathrm{Co}^{\mathrm{II}}$–SQ–X	1.883	1.871	2.352	2.354	1.929	1.928
	${}_{\mathrm{HS}}\mathrm{Co}^{\mathrm{II}}$–SQ–X	2.041	2.029	2.354	2.371	2.037	2.038
II (n = 4)	${}_{\mathrm{LS}}\mathrm{Co}^{\mathrm{II}}$–SQ–X	1.881	1.873	2.350	2.354	1.929	1.928
	${}_{\mathrm{HS}}\mathrm{Co}^{\mathrm{II}}$–SQ–X	2.040	2.029	2.356	2.369	2.037	2.037
III (n = 2)	${}_{\mathrm{LS}}\mathrm{Co}^{\mathrm{III}}$–Cat–X	1.875	1.895	2.013	1.926	1.950	2.051
	${}_{\mathrm{HS}}\mathrm{Co}^{\mathrm{II}}$–SQ–X	2.078	2.048	2.255	2.154	2.132	2.177
III (n = 3)	${}_{\mathrm{LS}}\mathrm{Co}^{\mathrm{III}}$–Cat–X	1.875	1.894	2.010	1.928	1.950	2.054
	${}_{\mathrm{HS}}\mathrm{Co}^{\mathrm{II}}$–SQ–X	2.082	2.042	2.258	2.157	2.131	2.177
III (n = 4)	${}_{\mathrm{LS}}\mathrm{Co}^{\mathrm{III}}$–Cat–X	1.874	1.896	2.012	1.927	1.949	2.053
	${}_{\mathrm{HS}}\mathrm{Co}^{\mathrm{II}}$–SQ–X	2.084	2.041	2.198	2.183	2.137	2.169
IV (n = 2)	${}_{\mathrm{LS}}\mathrm{Co}^{\mathrm{III}}$–Cat–X	1.871	1.885	2.016	2.018	1.949	2.060
	${}_{\mathrm{HS}}\mathrm{Co}^{\mathrm{II}}$–SQ–X	2.075	2.047	2.242	2.286	2.117	2.178
IV (n = 3)	${}_{\mathrm{LS}}\mathrm{Co}^{\mathrm{III}}$–Cat–X	1.871	1.888	2.019	2.018	1.950	2.060
	${}_{\mathrm{HS}}\mathrm{Co}^{\mathrm{II}}$–SQ–X	2.083	2.041	2.307	2.227	2.117	2.173
IV (n = 4)	${}_{\mathrm{LS}}\mathrm{Co}^{\mathrm{III}}$–Cat–X	1.870	1.889	2.019	2.020	1.950	2.059
	${}_{\mathrm{HS}}\mathrm{Co}^{\mathrm{II}}$–SQ–X	2.080	2.048	2.304	2.221	2.119	2.170

* The atoms were enumerated according to Scheme 3.

for the ${}_{\mathrm{LS}}\mathrm{Co}^{\mathrm{II}}$–SQ–X isomers. It should be mentioned that the exchange interactions between the organic radicals (J_3) weaken with an increase in the triangulene fragment size (Table 3). This tendency is caused by the delocalization of lone electrons of the polycycle on going from complex **I** (n = 2) bearing one electron on the X fragment to compound **I** (n = 4) in which the organosilicon moiety contains three electrons. It can be concluded that the insertion of radical X exerts no effect on the character and strength of the exchange between the divalent metal ion and SQ [50, 51]. At the same time, the presence of the polycyclic fragment in the molecule favors the formation of additional exchange channels.

The theoretical study of complexes **III** (n = 2–4) predicts the energy preference of the low-spin ${}_{\mathrm{LS}}\mathrm{Co}^{\mathrm{III}}$–Cat–X isomers (Fig. 1, Table 2). As in the considered above systems of compounds **I** and **II**, the variation of the polycyclic radical size exerts no effect on the geometric (Table 1) and energy (Table 2) characteristics of the electromers: the high-spin structures ${}_{\mathrm{HS}}\mathrm{Co}^{\mathrm{II}}$–SQ–X of compounds **III** (n = 2–4) are destabilized relative to the ground states ${}_{\mathrm{LS}}\mathrm{Co}^{\mathrm{III}}$–Cat–X by 8.4–8.7 kcal/mol. The calculated values of ΔE allow one to expect VT transitions with low conversions. As in the previously studied *o*-benzoquinone cobalt complexes with the tris(2-pyridylmethyl)amine derivatives [51, 53, 56, 74], in the ${}_{\mathrm{HS}}\mathrm{Co}^{\mathrm{II}}$–SQ–X electromers of

Table 2. Spin (S), total energy (E), relative energy (ΔE), and spin density on the metal center $\left(q_{\mathrm{s}}^{\mathrm{Co}}\right)$ in the electromers of complexes **I**–**IV** (n = 2–4) calculated by the DFT UTPSSh/6-311++G(d,p) method

Complex	Electromer	S	E, a.u.	ΔE, kcal/mol	$q_{\mathrm{s}}^{\mathrm{Co}}$
I (n = 2)	$_{\mathrm{LS}}\mathrm{Co}^{\mathrm{III}}$–Cat–X	1/2	–5711.654371	0.0	0.00
	$_{\mathrm{HS}}\mathrm{Co}^{\mathrm{II}}$–SQ–X	5/2	–5711.635697	11.7	2.62
I (n = 3)	$_{\mathrm{LS}}\mathrm{Co}^{\mathrm{III}}$–Cat–X	1	–7062.105189	0.0	0.00
	$_{\mathrm{HS}}\mathrm{Co}^{\mathrm{II}}$–SQ–X	3	–7062.086342	11.8	2.63
I (n = 4)	$_{\mathrm{LS}}\mathrm{Co}^{\mathrm{III}}$–Cat–X	3/2	–8740.208385	0.0	0.00
	$_{\mathrm{HS}}\mathrm{Co}^{\mathrm{II}}$–SQ–X	7/2	–8740.189508	11.8	2.63
II (n = 2)	$_{\mathrm{LS}}\mathrm{Co}^{\mathrm{II}}$–SQ–X	3/2	–5790.286545	0.0	1.26
	$_{\mathrm{HS}}\mathrm{Co}^{\mathrm{II}}$–SQ–X	5/2	–5790.273984	7.9	2.59
II (n = 3)	$_{\mathrm{LS}}\mathrm{Co}^{\mathrm{II}}$–SQ–X	2	–7140.737126	0.0	1.27
	$_{\mathrm{HS}}\mathrm{Co}^{\mathrm{II}}$–SQ–X	3	–7140.724473	7.9	2.59
II (n = 4)	$_{\mathrm{LS}}\mathrm{Co}^{\mathrm{II}}$–SQ–X	5/2	–8818.840317	0.0	1.25
	$_{\mathrm{HS}}\mathrm{Co}^{\mathrm{II}}$–SQ–X	7/2	–8818.827682	7.9	2.60
III (n = 2)	$_{\mathrm{LS}}\mathrm{Co}^{\mathrm{III}}$–Cat–X	1/2	–5708.043783	0.0	0.00
	$_{\mathrm{HS}}\mathrm{Co}^{\mathrm{II}}$–SQ–X	5/2	–5708.030305	8.5	2.51
III (n = 3)	$_{\mathrm{LS}}\mathrm{Co}^{\mathrm{III}}$–Cat–X	1	–7058.494546	0.0	0.00
	$_{\mathrm{HS}}\mathrm{Co}^{\mathrm{II}}$–SQ–X	3	–7058.480643	8.7	2.62
III (n = 4)	$_{\mathrm{LS}}\mathrm{Co}^{\mathrm{III}}$–Cat–X	3/2	–8736.598216	0.0	0.00
	$_{\mathrm{HS}}\mathrm{Co}^{\mathrm{II}}$–SQ–X	7/2	–8736.584781	8.4	2.61
IV (n = 2)	$_{\mathrm{LS}}\mathrm{Co}^{\mathrm{III}}$–Cat–X	1/2	–5747.364131	0.0	0.00
	$_{\mathrm{HS}}\mathrm{Co}^{\mathrm{II}}$–SQ–X	5/2	–5747.360056	2.6	2.57
IV (n = 3)	$_{\mathrm{LS}}\mathrm{Co}^{\mathrm{III}}$–Cat–X	1	–7097.815103	0.0	0.00
	$_{\mathrm{HS}}\mathrm{Co}^{\mathrm{II}}$–SQ–X	3	–7097.810785	2.7	2.55
IV (n = 4)	$_{\mathrm{LS}}\mathrm{Co}^{\mathrm{III}}$–Cat–X	3/2	–8775.918606	0.0	0.00
	$_{\mathrm{HS}}\mathrm{Co}^{\mathrm{II}}$–SQ–X	7/2	–8775.914163	2.8	2.59

compounds **III** (n = 2–4) the metal center and SQ radical interact ferromagnetically. The character and strength of magnetic coupling in the SQ–X pair are analogous to those predicted in complexes **I** and **II** (n = 2–4), and an exchange between the lone electrons of the cobalt ion and organosilicon fragment is nearly absent (Table 3).

The calculation results for compounds **I** and **III** (n = 2–4) indicate an increase in the energy gap ΔE (Table 2) over the values predicted for the similarly built derivatives containing no polycyclic radicals [50, 51, 53, 55, 56]. It is shown [49, 53, 74] that the presence of electron-active substituents in the quinone ring of the *o*-benzoquinone cobalt complexes with tetradentate N-donor ligands makes it possible to control the difference in energies between the electromers, which predetermines the probability of the redox process to occur. The cobalt complex with 3,5-di-*tert*-butyl-*o*-benzoquinone and TPA bearing one methyl group in each pyridine ring is known [47, 51] to exist as the high-spin electromer $_{\mathrm{HS}}\mathrm{Co}^{\mathrm{II}}$–SQ due to the destabilization of the $_{\mathrm{LS}}\mathrm{Co}^{\mathrm{III}}$–Cat form. It can be expected that the observed enhancement of the stability of the low-spin state upon the insertion of an organosilicon radical would favor VT rearrangements to occur in compounds **IV** (n = 2–4) with tris(2-pyridylmethyl)amine bearing three CH_3 substituents (Scheme 2). In order to check this hypothesis, we performed computer modeling of the electronic structures and magnetic properties of these complexes.

Table 3. Exchange interaction parameters (J, cm^{-1}) in the $_{\text{LS}}\text{Co}^{\text{II}}$–SQ–X and $_{\text{HS}}\text{Co}^{\text{II}}$–SQ–X electromers of complexes **I**–**IV** (n = 2–4) calculated by the DFT UTPSSh/6-311++G(d,p) method

Complex	Electromer	J_1*	J_2	J_3
I (n = 2)	$_{\text{HS}}\text{Co}^{\text{II}}$–SQ–X	–98	2	197
I (n = 3)	$_{\text{HS}}\text{Co}^{\text{II}}$–SQ–X	–96	1	131
I (n = 4)	$_{\text{HS}}\text{Co}^{\text{II}}$–SQ–X	–98	1	80
II (n = 2)	$_{\text{LS}}\text{Co}^{\text{II}}$–SQ–X	271	–9	155
	$_{\text{HS}}\text{Co}^{\text{II}}$–SQ–X	–43	–6	181
II (n = 3)	$_{\text{LS}}\text{Co}^{\text{II}}$–SQ–X	264	–8	102
	$_{\text{HS}}\text{Co}^{\text{II}}$–SQ–X	–46	–4	117
II (n = 4)	$_{\text{LS}}\text{Co}^{\text{II}}$–SQ–X	258	–6	64
	$_{\text{HS}}\text{Co}^{\text{II}}$–SQ–X	–49	–2	72
III (n = 2)	$_{\text{HS}}\text{Co}^{\text{II}}$–SQ–X	81	0	127
III (n = 3)	$_{\text{HS}}\text{Co}^{\text{II}}$–SQ–X	78	–1	78
III (n = 4)	$_{\text{HS}}\text{Co}^{\text{II}}$–SQ–X	77	–1	47
IV (n = 2)	$_{\text{HS}}\text{Co}^{\text{II}}$–SQ–X	85	–6	155
IV (n = 3)	$_{\text{HS}}\text{Co}^{\text{II}}$–SQ–X	86	2	80
IV (n = 4)	$_{\text{HS}}\text{Co}^{\text{II}}$–SQ–X	82	–4	65

* J_1 corresponds to the exchange between Co$^{\text{II}}$ and SQ, J_2 corresponds to the exchange between Co$^{\text{II}}$ and X, and J_3 corresponds to the exchange between SQ and X.

The spin density distribution in the electromers of compounds **IV** (n = 2–4) is similar to that found for complexes **III** (n = 2–4) (Fig. 1). A comparison of the calculated geometric parameters of the discussed systems indicates that an additional bulky alkyl substituent in the pyridine ring results in the elongation of the Fe–N(2) distances and a slight change in the coordination bond lengths in compounds **IV** (n = 2–4) (Table 1). The stability of the low-spin electromers $_{\text{LS}}\text{Co}^{\text{III}}$–Cat–X decreases compared to that of complexes **III** (n = 2–4), because short interatomic Fe–N distances cannot be formed (Table 2). However, unlike the earlier studied *o*-benzoquinone cobalt derivatives with trimethyl-substituted TPA [47, 51], in coordination compounds **IV** (n = 2–4) the $_{\text{LS}}\text{Co}^{\text{III}}$–Cat–X electromers correspond to the ground state. This fact provides prerequisites for VT transitions to occur. Indeed, the differences in energies between the $_{\text{LS}}\text{Co}^{\text{III}}$–Cat–X and $_{\text{HS}}\text{Co}^{\text{II}}$–SQ–X structures are 2.6–2.8 kcal/mol (Table 2), indicating that VT transitions can occur at ambient temperatures. Depending on the number of six-membered rings in the organosilicon radical, the $_{\text{LS}}\text{Co}^{\text{III}}$–Cat–X electromers are characterized by spin states S equal to 1/2 (n = 2), 1 (n = 3), and 3/2 (n = 4). The retention of the possibly maximum total spin S is expected in the high-spin structures owing to the ferromagnetic exchange interactions (Table 3). Therefore, the predicted VT rearrangements would be accompanied by a change in the magnetic properties and, hence, compounds **IV** (n = 2–4) can be considered as a basis for molecular switches.

Thus, the molecules capable of manifesting the spin state switching mechanisms (spin-crossover and valence tautomerism) were revealed by the quantum-chemical study of the cobalt complexes designed from *o*-benzoquinones bearing triangulene organosilicon substituents and ancillary N-donor ligands. The polycyclic radical and strong ferromagnetic interactions provide paramagnetism of all studied molecules. It is shown that the energy characteristics of the electromers of compounds **I**–**IV** (n = 2–4) are independent of the size of the organosilicon fragment and controlled by structural features of the tetradentate nitrogen-containing bases. An advantage of the proposed systems over the earlier studied compounds with the acene fragments [82–84] is paramagnetism of all electromeric forms due to the presence of ferromagnetically bound electrons in the triangulene radical. In addition, complexes **I**–**IV** have a higher total spin that can be additionally increased due to the expansion of the polycyclic moiety, which would enrich functional possibilities of similar systems.

FUNDING

This work was supported by the Ministry of Science and Higher Education of the Russian Federation (state assignment in the field of scientific activity, project no. 0852-2020-0031).

CONFLICT OF INTEREST

The authors declare that they have no conflicts of interest.

REFERENCES

1. *Molecular Switches*, Feringa B.L. and Browne W.R., Eds., Weinheim: Wiley, 2011.
2. Witt, A., Heinemann, F.W., Sproules, S., and Khusniyarov, M.M., *Chem.-Eur. J.*, 2014, vol. 20, no. 35, p. 11149.
3. Sato, O., *Nature Chem.*, 2016, vol. 8, no. 7, p. 644.
4. Senthil Kumar, K. and Ruben, M., *Coord. Chem. Rev.*, 2017, vol. 346, p. 176.
5. Drath, O. and Boskovic, C., *Coord. Chem. Rev.*, 2018, vol. 375, p. 256.
6. Starikova, A.A. and Minkin, V.I., *Russ. Chem. Rev.*, 2018, vol. 87, no. 11, p. 1049. https://doi.org/10.1070/RCR4837
7. Coronado, E., *Nat. Rev. Mater.*, 2020, vol. 5, p. 87.
8. Zolotukhin, A.A., Bubnov, M.P., Cherkasov, V.K., et al., *Russ. J. Coord. Chem.*, 2018, vol. 44, no. 4, p. 272. https://doi.org/10.1134/S1070328418040085
9. Chegerev, M.G. and Starikova, A.A., *Eur. J. Inorg. Chem.*, 2021, no. 27, p. 2684.
10. Bally, T., *Nature Chem.*, 2010, vol. 2, no. 3, p. 165.
11. Minkin, V.I., *Russ. Chem. Bull.*, 2008, vol. 57, no. 4, p. 687. https://doi.org/10.1007/s11172-008-0111-y
12. Dei, A. and Sorace, L., *Appl. Magn. Reson.*, 2010, vol. 38, no. 2, p. 139.
13. Timco, G.A., Carretta, S., Troiani, F., et al., *Nat. Nanotechnol.*, 2009, vol. 4, no. 3, p. 173.
14. Aromí, G., Aguilá, D., Gamez, P., et al., *Chem. Soc. Rev.*, 2012, vol. 41, no. 2, p. 537.
15. Demir, S., Jeon, I.-R., Long, J.R., and Harris, T.D., *Coord. Chem. Rev.*, 2015, vol. 289-290, p. 149.
16. Venkataramani, S., Jana, U., Dommaschk, M., et al., *Science*, 2011, vol. 331, no. 6016, p. 445.
17. Mörtel, M., Seller, M., Heinemann, F.W., and Khusniyarov, M.M., *Dalton Trans.*, 2020, vol. 49, no. 48, p. 17532.
18. Ovcharenko, V.I. and Kuznetsova, O.V., *Russ. Chem. Rev.*, 2020, vol. 89, no. 11, p. 1261. https://doi.org/10.1070/RCR4981
19. Nikovskiy, I., Polezhaev, A., Novikov, V., et al., *Chem.-Eur. J.*, 2020, vol. 26, no. 15, p. 5629.
20. Nadurata, V.L. and Boskovic, C., *Inorg. Chem. Front.*, 2021, vol. 8, no. 7, p. 1840.
21. *Spin Crossover in Transition Metal Compounds I,* Gütlich, P. and Goodwin, H.A., Eds., Berlin: Springer, 2004, vol. 233.
22. *Spin-Crossover Materials: Properties and Applications*, Halcrow, M.A., Ed., Chichester: Wiley, 2013.
23. Hauser, A., *Coord. Chem. Rev.*, 1991, vol. 111, p. 275.
24. Hauser, A., Enachescu, C., Daku, M.L., et al., *Coord. Chem. Rev.*, 2006, vol. 250, p. 1642.
25. Halcrow, M.A., *Polyhedron*, 2007, vol. 26, no. 14, p. 3523.
26. Harding, D.J., Harding, P., and Phonsri, W., *Coord. Chem. Rev.*, 2016, vol. 313, p. 38.
27. Khusniyarov, M.M., *Chem.-Eur. J.*, 2016, vol. 22, no. 43, p. 15178.
28. Krivokapic, I., Zerara, M., Daku, M.L., et al., *Coord. Chem. Rev.*, 2007, vol. 251, p. 364.
29. Vologzhanina, A.V., Belov, A.S., Novikov, V.V., et al., *Inorg. Chem.*, 2015, vol. 54, no. 12, p. 5827.
30. Taylor, R.A., Lough, A.J., and Lemaire, M.T., *J. Mater. Chem.*, 2016, vol. 4, no. 3, p. 455.
31. Evangelio, E. and Ruiz-Molina, D., *Eur. J. Inorg. Chem.*, 2005, no. 15, p. 2957.
32. Tezgerevska, T., Alley, K.G., and Boskovic, C., *Coord. Chem. Rev.*, 2014, vol. 268, p. 23.
33. Rajput, A., Sharma, A.K., Barman, S.K., et al., *Coord. Chem. Rev.*, 2020, vol. 414, p. 213240.
34. Fedushkin, I., Maslova, O., Morozov, A., et al., *Angew. Chem., Int. Ed. Engl.*, 2012, vol. 51, no. 42, p. 10584.
35. Chegerev, M.G., Starikova, A.A., Piskunov, A.V., and Cherkasov, V.K., *Eur. J. Inorg. Chem.*, 2016, no. 2, p. 252.
36. Chegerev, M.G., Piskunov, A.V., Starikova, A.A., et al., *Eur. J. Inorg. Chem.*, 2018, no. 9, p. 1087.
37. Kirk, M.L. and Shultz, D.A., *Coord. Chem. Rev.*, 2013, vol. 257, no. 1, p. 218.
38. Tichnell, C.R., Shultz, D.A., Popescu, C.V., et al., *Inorg. Chem.*, 2015, vol. 54, no. 9, p. 4466.
39. Bubnov, M., Cherkasova, A., Teplova, I., et al., *Polyhedron*, 2016, vol. 119, p. 317.
40. Artiukhova, N.A., Romanenko, G.V., Bogomyakov, A.S., et al., *J. Mater. Chem. C*, 2016, vol. 4, no. 47, p. 11157.
41. Bubnov, M.P., Teplova, I.A., Kopylova, E.A., et al., *Inorg. Chem.*, 2017, vol. 56, no. 5, p. 2426.
42. Zolotukhin, A.A., Bubnov, M.P., Arapova, A.V., et al., *Inorg. Chem.*, 2017, vol. 56, no. 24, p. 14751.
43. Cherkasova, A.V., Kozhanov, K.A., Zolotukhin, A.A., et al., *Russ. J. Coord. Chem.*, 2019, vol. 45, no. 7, p. 489. https://doi.org/10.1134/S1070328419070029
44. Protasenko, N.A., Poddel'sky, A.I., Bogomyakov, A.S., et al., *Inorg. Chim. Acta*, 2019, vol. 489, p. 1.
45. Kuznetsova, O.V., Romanenko, G.V., Bogomyakov, A.S., and Ovcharenko, V.I., *Russ. J. Coord. Chem.*, 2020, vol. 46, no. 8, p. 521. https://doi.org/10.1134/S1070328420070039
46. Maryunina, K., Yamaguchi, K., Nishihara, S., et al., *Cryst. Growth Des.*, 2020, vol. 20, no. 4, p. 2796.
47. Beni, A., Dei, A., Laschi, S., et al., *Chem.-Eur. J.*, 2008, vol. 14, no. 6, p. 1804.
48. Graf, M., Wolmershäuser, G., Kelm, H., et al., *Angew. Chem., Int. Ed. Engl.*, 2010, vol. 49, no. 5, p. 950.
49. Gransbury, G.K., Boulon, M.-E., Petrie, S., et al., *Inorg. Chem.*, 2019, vol. 58, no. 7, p. 4230.

50. Tezgerevska, T., Rousset, E., Gable, R.W., et al., *Dalton Trans.*, 2019, vol. 48, no. 31, p. 11674.
51. Starikova, A.A., Chegerev, M.G., and Starikov, A.G., *Russ. J. Coord. Chem.*, 2020, vol. 46, no. 3, p. 193. https://doi.org/10.1134/S1070328420030070
52. Starikov, A.G., Starikova, A.A., and Minkin, V.I., *Dokl. Chem.*, 2016, vol. 467, no. 1, p. 83. https://doi.org/10.1134/S0012500816030113
53. Starikova, A.A., Chegerev, M.G., Starikov, A.G., and Minkin, V.I., *Comp. Theor. Chem.*, 2018, vol. 1124, p. 15.
54. Starikov, A.G., Chegerev, M.G., and Starikova, A.A., *Struct. Chem.*, 2020, vol. 31, no. 1, p. 37.
55. Minkin, V.I., Starikova, A.A., Chegerev, M.G., and Starikov, A.G., *Russ. J. Coord. Chem.*, 2020, vol. 46, no. 6, p. 371. https://doi.org/10.1134/S1070328420060068
56. Starikova, A.A., Chegerev, M.G., and Starikov, A.G., *Chem. Phys. Lett.*, 2021, vol. 762, p. 138128.
57. Starikov, A.G., Starikova, A.A., Minyaev, R.M., et al., *Chem. Phys. Lett.*, 2020, vol. 740, p. 137073.
58. Minkin, V.I., Starikova, A.A., Chegerev, M.G., and Starikov, A.G., *Dokl. Chem.*, 2020, vol. 494, no. 2, p. 149. https://doi.org/10.1134/S001250082010002X
59. Chegerev, M.G., Starikova, A.A., Starikov, A.G., and Minkin, V.I., *Russ. J. Gen. Chem.*, 2020, vol. 90, no. 12, p. 2312. https://doi.org/10.1134/S1070363220120142
60. Starikov, A.G., Chegerev, M.G., Starikova, A.A., and Minkin, V.I., *Russ. Chem. Bull*, 2021, vol. 70, no. 2, p. 309. https://doi.org/10.1007/s11172-021-3086-6
61. Starikova, A.A., Minyaev, R.M., and Minkin, V.I., *Russ. Chem. Bull.*, 2014, vol. 63, no. 4, p. 812. https://doi.org/10.1007/s11172-014-0514-x
62. Starikova, A.A., Minkin, V.I., and Starikov, A.G., *Mendeleev Commun.*, 2014, vol. 24, no. 6, p. 329.
63. Fokin, S.V., Fursova, E.Yu., Letyagin, G.A., et al., *J. Struct. Chem.*, 2020, vol. 61, no. 4, p. 541. https://doi.org/10.1134/S002247662004006X
64. *Polyarenes I,* Siegel, J.S. and Wu, Y.-T., Eds., Berlin: Springer, 2014.
65. Gapurenko, O.A., Starikov, A.G., Minyaev, R.M., and Minkin, V.I., *J. Comput. Chem.*, 2015, vol. 36, no. 29, p. 2193.
66. Ovchinnikov, A.A., *Theor. Chem. Acc.*, 1978, vol. 47, p. 297.
67. *Stable Radicals: Fundamental and Applied Aspects of Odd-Electron Compounds*, Hicks, R., Ed., Chichester: Wiley, 2011.
68. Frisch, M.J., Trucks, G.W., Schlegel, H.B., et al., *Gaussian 16, Revision C. 01*, Wallingford: Gaussian, 2016.
69. Tao, J.M., Perdew, J.P., Staroverov, V.N., and Scuseria, G.E., *Phys. Rev. Lett.*, 2003, vol. 91, no. 14, p. 146401.
70. Staroverov, V.N., Scuseria, G.E., Tao, J., and Perdew, J.P., *J. Chem. Phys.*, 2003, vol. 119, no. 23, p. 12129.
71. Cirera, J. and Ruiz, E., *J. Mater. Chem.*, 2015, vol. 3, no. 30, p. 7954.
72. Cirera, J., Via-Nadal, M., and Ruiz, E., *Inorg. Chem.*, 2018, vol. 57, no. 22, p. 14097.
73. Starikov, A.G., Starikova, A.A., Chegerev, M.G., and Minkin, V.I., *Russ. J. Coord. Chem.*, 2019, vol. 45, no. 2, p. 105. https://doi.org/10.1134/S1070328419020088
74. Gransbury, G.K., Livesay, B.N., Janetzki, J.T., et al., *J. Am. Chem. Soc.*, 2020, vol. 142, no. 24, p. 10692.
75. Minkin, V.I., Starikov, A.G., and Starikova, A.A., *Pure Appl. Chem.*, 2018, vol. 90, no. 5, p. 811.
76. Noodleman, L., *J. Chem. Phys.*, 1981, vol. 74, no. 10, p. 5737.
77. Shoji, M., Koizumi, K., Kitagawa, Y., et al., Chem. Phys. Lett., 2006, vol. 432, nos. 1–3, p. 343.
78. Chemcraft. Version 1.8. 2014. http://www.chemcraftprog.com.
79. Melle-Franco, M., *Chem. Commun.*, 2015, vol. 51, no. 25, p. 5387.
80. Sharma, V., Som, N., Dabhi, S.D., and Jha, P.K., *ChemSelect*, 2018, vol. 3, no. 8, p. 2390.
81. Minkin, V.I., Starikov, A.G., Starikova, A.A., et al., *Phys. Chem. Chem. Phys.*, 2020, vol. 22, no. 3, p. 1288.
82. Minkin, V.I., Starikov, A.G., Starikova, A.A., et al., *Dalton Trans.*, 2018, vol. 47, no. 44, p. 15948.
83. Starikova, A.A., Metelitsa, E.A., and Minkin, V.I., *Russ. J. Coord. Chem.*, 2019, vol. 45, no. 6, p. 411. https://doi.org/10.1134/S1070328419060095
84. Minkin, V.I., Starikov, A.G., and Starikova, A.A., *J. Phys. Chem. A*, 2021, vol. 125, no. 30, p. 6562.

Translated by E. Yablonskaya